Larrosa, N. O., Lopez-Crespo, P., & Ainsworth, R. A. (2018). An efficient procedure for reducing in-line-inspection datasets for structural integrity assessments. *Theoretical and Applied Fracture Mechanics*, *93*, 79-87. https://doi.org/10.1016/j.tafmec.2017.07.005

Peer reviewed version

An efficient procedure for reducing in-line-inspection datasets for structural integrity assessments

N.O. Larrosa, P. Lopez-Crespo, R.A. Ainsworth

PII: S0167-8442(17)30112-X
DOI: http://dx.doi.org/10.1016/j.tafmec.2017.07.005
Reference: TAFMEC 1910

To appear in: *Theoretical and Applied Fracture Mechanics*

Received Date: 8 March 2017
Accepted Date: 6 July 2017

Please cite this article as: N.O. Larrosa, P. Lopez-Crespo, R.A. Ainsworth, An efficient procedure for reducing in-line-inspection datasets for structural integrity assessments, *Theoretical and Applied Fracture Mechanics* (2017), doi: http://dx.doi.org/10.1016/j.tafmec.2017.07.005

An efficient procedure for reducing in-line-inspection datasets for structural integrity assessments.

N. O. Larrosa[a,b,c 1], P. Lopez-Crespo[a,b], R.A. Ainsworth[d]

[a] *Department of Civil and Materials Engineering, University of Malaga, C/Dr. Ortiz Ramos s/n, 29071, Malaga, Spain.*

[b] *Department of Mechanical Engineering, University of Bristol, Queen's Building, University Walk, Bristol, BS8 1TR, UK*

[c] *School of Materials, The University of Manchester, Manchester M13 9PL, United Kingdom.*

[d] *School of Mechanical, Aerospace & Civil Engineering, The University of Manchester, Manchester M13 9PL, United Kingdom.*

Abstract

In-line inspection (ILI) has become a routine procedure in the Oil and Gas industry for performing cost-effective pipeline integrity assessments, allowing continuing monitoring and providing a basis for informed decisions in terms of repair, maintenance or a change to the operating conditions. The amount of ILI data is however immense and dealing with these data from a fitness-for-service point of view poses a significant challenge to the industry. Thus, smart methods for using ILI data in the assessment of the integrity of oil and gas transmission pipelines are essential. The aim of this paper is to propose a screening approach for reducing the amount of ILI inspection data requiring detailed structural integrity assessment. The screening approach has two main stages: (I) a geometry based filter assessing the shape of the flaw and (II) an elastic stress based filter that uses the point method, as in the Theory of Critical Distances (TCD), to identify the most severe flaws. The methodology uses the outputs from ILI (dimensions of flaws, orientation and distance from starting point) to generate a visualisation of the pits within the pipeline, a ranking of pits in terms of sphericity (roundness) and depth, to evaluate pit density and generate the models for finite element analysis. The method was tested on actual ILI data, where the number of pits in a 12.75 inch riser of 11 km length was reduced significantly (i.e. two/three orders of magnitude), such reduction depending on the level of conservatism introduced by the analyst. The tool will allow Oil and Gas owners and operators to reduce the immense amount of data obtained during pigging to a much less time-consuming set for flaw assessment.

Key words: In-line inspection data, Screening methodology, Pitting corrosion, Sphericity, Theory of Critical Distances, Fatigue, Fracture

Nomenclature

$\Delta\sigma_{FL}$	Plain fatigue limit
ΔK_{th}	Threshold stress intensity factor range
Ψ	Sphericity
σ_0	Inherent material strength
a	Flaw depth
B	Pipe thickness
c	Flaw half-width
J	J-integral
K	Stress intensity factor
K_{IC}	Plane strain fracture toughness
L	Material characteristic length
l	Flaw half-length
r_0	Pipe outer radius

1 Introduction

Corrosion control is within the responsibility of pipeline owners and operators. Knowing the condition of a pipeline is an essential prerequisite for being able to devise an appropriate set of measures and activities to manage its integrity. Through ILI tools and field nondestructive examination (NDE), pipeline operators have access to a wealth of data, providing information about anomalies for extensive pipelines. These tools have become a valuable asset to the industry for pipeline inspection and integrity management, and for characterising the geometry of flaws in the pipe wall. Such data can be used in conjunction with proper failure assessment models to allow for structural characterisation and life estimation.

Various in-line inspections techniques are used to characterise the geometry of detected mechanical and corrosion damage and each tool has its own advantages and disadvantages [1]. Advances in ILI technologies have provided an opportunity to leverage structural integrity assessments, by means of continuous improvement of defect detection data accuracy and reduced uncertainty in defect location and sizing [2]. These technologies have acted as driving forces

[1] e-mail: nicolas.larrosa@manchester.ac.uk

for the development of a number of procedures for assessing metal loss and cracks in pipelines [3].

Standard procedures like ASME B31G[4], API 579[5] or DNV-RP-F101 [6] are used in the Oil and Gas (O&G) industry to evaluate the remaining strength of corroded pipelines based on plastic collapse criteria as it has been recognised that plastic flow is the predominant failure mechanism in ductile pipeline steels with corrosion defects, gouges or dents in which the defect can be categorised as a smooth local thinned area (LTA). However, these procedures are not intended to cover applications where the component contains notch-like (3D) and/or crack-like (2D) flaws subject to significant fatigue loading, or when fracture is likely to initiate from the flaw. For example, manufacturing defects in pipeline longitudinal welds that are in cyclic service can experience growth by fatigue. In addition, pitting corrosion is the most common form of corrosion observed in O&G transmission pipelines. Corrosion pits have been shown to act as mechanical stress raisers promoting crack initiation and ductile tearing of the defect through the remaining ligament.

In cases where detected anomalies cannot be considered as LTA, Fitness-for-service (FFS) assessment procedures, such as API RP 1176, API 579 and BS 7910 [7], provide recommendations based on fracture mechanics and evaluate the integrity of structures by considering detected or postulated anomalies as crack-like defects. For the assessment of notch-like defects, such as localised corrosion (pitting), which are three-dimensional in nature, the application of these approaches requires the simplification and re-characterisation of these defects into sharp cracks, both because they can be analysed by linear elastic fracture mechanics (LEFM) or elastic plastic fracture mechanics (EPFM) and also because this assumption represents the worst case scenario from a FFS point of view. Figure 1 shows a schematic of the expected burst pressure as a function of the notch acuity and the values used in FFS assessment procedures used in the calculation methods to find a reduced Maximum Allowable Working Pressure (MAWP). In some cases, however, this can lead to overly conservative results and effort is currently focused on improving assessment methodologies for non-sharp defects [8–18,32] to better address the damage mechanism involved, e.g. plastic collapse or fracture, for more efficient pipeline integrity management. Methodologies that consider the constraint conditions at the defect surroundings, either explicitly [19,20] or implicitly [21,23–25], allow for a more complete characterisation of the stress and strain fields and for an improved capability to assess the integrity of the structure [22,26,27].

Despite recent advances in analytical software and computing power, performing and interpreting FFS assessments of large data sets obtained during ILI from thousands of kilometres of pipelines is time consuming and expensive. It is therefore important to reduce ILI datasets to focus attention on the most severe flaws. This allows a reduction in the costs, time and effort dedicated to

the evaluation of remaining life and/or inspection intervals.

This paper presents a novel methodology to reduce the amount of ILI data for FFS assessments and provides a basis for the application of more advanced and accurate routes to reduce the number of flaws to those considered to be most detrimental. The proposed approach includes a rendering tool for visualisation of anomalies within pipelines and a simple-to-apply procedure for ILI inspection data screening. The paper focuses attention particularly on pitting data from an oil and gas pipeline but the proposed approach can be used to evaluate gouges, dents or any non-sharp flaw in industrial components affected by corrosion, such as naval, petrochemical, aerospace and marine structures. The overall methodology proposed in this paper has three basic steps: 1) a graphical geometry based filter; 2) an elastic stress-based filter that uses the Theory of Critical Distances (TCD); and 3) the application of failure models required for life estimation.

The application of advanced failure models in Step 3 depends on the failure mechanisms involved in the analysis, e.g fatigue, corrosion-fatigue, fracture, etc. This step is devoted to the analysis of the filtered data as outcome from Step 2. In this paper, attention is only focused on the screening methodology of Steps 1 and 2.

2 Screening procedure

Inspection of pipelines is performed periodically either by nondestructive test (NDT) techniques, or non-destructive test technologies used on intelligent in-line inspection (ILI) tools to locate and identify anomalies. The information typically provided by ILI tools consists of geometric features regarding flaws and anomalies, such as length, depth, width, circumferential position and longitudinal position. Although these techniques allow a three-dimensional characterisation of defects, in integrity assessments it is common to recharacterise detected flaws into 2D crack-like defects. This is performed due to the lack of widely accepted methodologies and recommendations in assessment procedures [5,7] on how to deal with volumetric defects. As a result, detected flaws are considered to be infinitely sharp and fracture mechanics is utilised for characterising their severity. Assuming volumetric defects as 2D sharp cracks can lead to a pessimistic assessment of the remnant life of the structure. The portion of life in which a localised corrosion defect (a pit) transitions to a crack is neglected by this characterisation approach. The pit-to-crack transition period depends on several factors, of which the pit macro-topography [28–31] plays a major role, thus it is fundamental to include it in the analysis.

In order to obtain the full benefit of ILI techniques, it is necessary to consider

the actual geometry of defects in integrity assessments. For time and cost efficiency, integrity assessments of pipelines containing large number of defects would benefit from methodologies that reduce the number of defects requiring detailed analysis [8–18,32].

The screening approach proposed in this paper aims to address the lack of recommendations in defect integrity assessment procedures regarding the analysis and characterisation of non-sharp defects and the relative criticality within the structure. The simplicity of the approach lies in the fact that defects are compared based on their geometrical features and ranked based on linear elastic FEA.

2.1 Geometry based filter

The first step in the screening approach is a *Geometry based filter*, which involves processing all the data and calculating the sphericity (Ψ) of each of the flaws detected during ILI. The sphericity [33] is a measure of roundness and is calculated as:

$$\Psi = \frac{\pi^{1/3}(6V)^{2/3}}{A} \tag{1}$$

thus it is the ratio of the surface area of a sphere of the same volume (V) as the defect to the actual surface area of the defect (A), assuming each defect as a smooth tri-axial ellipsoid (three axes have different lengths), as shown in Fig 2. Sphericity values range from 0 (flat, 2D defect) to 1 (perfect sphere, 3D defect).

The dimensions of the flaws (a, $2c$ and $2l$) are used to calculate V and A for each defect. The severity of all flaws is ranked in terms of a Ψ-a/B plot. Flaws that are considered more severe are deep flaws (high a/B) with low values of sphericity, that is flat or crack-like flaws. On the other hand, shallow non-sharp flaws are less detrimental to the integrity of the structure, Fig 1.

The second part of the *Geometry based filter* uses the projection of each defect in the axial and circumferential directions, where the relevant geometrical parameters are a/c and a/l respectively, see Fig 2. The approach assumes that, as for crack like-flaws, for a defect of given depth, the driving force ($J, K, CTOD$), increases with decreasing a/c and a/l. This is discussed in Section 4. Thus, for given a/B, flaws with the lowest values of a/c and a/l are selected for further analysis.

The *Geometry based filter* allows the user to select the most detrimental flaws within the structure. Specifically, the defects selected are those with the lowest sphericity, those that are deepest (highest a/B), and for given a/B those with

the lowest a/c and a/l. This is illustrated in Section 3. It is worth mentioning that in this paper the interaction of neighbouring defects is not addressed. This will be considered in future work.

For those flaws that are considered most severe in this step, the tool generates a render of the pipeline with the defects and the FEA model for posterior numerical analysis. Again, this is illustrated in Section 3. A sub-modeling approach in the Abaqus [34] environment has been set up for the sake of efficiency.

2.2 Theory of critical distances (TCD)

A rank of the flaws in terms of the varying severity of the elastic stress field is performed in Step 2 of the screening approach. The critical distance method [35] in its simplest version, i.e. the point method (PM), is applied. The PM is not used to calculate an absolute value of the fatigue/fracture resistance of the defective pipe but as a consistent methodology to compare and rank defects in terms of criticality. To do so, the maximum value of the opening stress at a distance $L/2$ from the tip of the flaw is calculated in this step, with L given as:

$$L = \frac{1}{\pi}\left(\frac{\Delta K_{th}}{\Delta \sigma_{FL}}\right)^2 \tag{2}$$

or

$$L = \frac{1}{\pi}\left(\frac{K_{IC}}{\sigma_0}\right)^2 \tag{3}$$

for fatigue [36] and fracture assessments [37], respectively. In the equations above, ΔK_{th} is the range of the threshold value of the stress intensity factor, $\Delta \sigma_{FL}$ is the plain material fatigue limit, K_{Ic} is the plane strain fracture toughness and σ_0 is the inherent material strength, which needs to be defined experimentally as reported in [37]. It will be seen in Section 3, however, that a precise value of L is not needed for the purposes of ranking flaws.

The value of stress for the defected component at failure is then calculated as:

$$\sigma_{cr}^{Pit} = \sigma_{cr}\left[\frac{\sigma_{\theta\theta}^{UN}}{\sigma_{\theta\theta}}\right]_{d=L/2} \tag{4}$$

where $\sigma_{\theta\theta}$ and $\sigma_{\theta\theta}^{UN}$ are the stress ahead of the defect tip and the membrane stress in the circumferential direction, respectively, and σ_{cr} is the critical stress for the non-defected material, with $\sigma_{cr} = \Delta\sigma_{FL}$ and $\sigma_{cr} = \sigma_0$ for fatigue and fracture assessments, respectively. Flaws exhibiting the lowest values of critical stress at the distance $L/2$ are considered potential threats to the integrity

of the component and require further analysis with more advances techniques. The application of elastic-plastic FEA together with fatigue/fracture damage models is considered as a potential method for life and fatigue/fracture strength assessment in Step 3 of the overall methodology. Progress in the development of a methodology for fatigue and fracture assessment of non-sharp defects has been reported recently [16,26,27,32] by the authors. However, as noted earlier, this stage is not considered in this paper.

3 Application of the procedure

A representative batch of data obtained during in-line inspection of a 12.75" (323.85mm) riser is analysed in what follows. The main characteristics of the component are shown in Table 1. The proposed approach is equally applicable to different loading cases (e.g., pure bending, internal pressure, combined pressure-bending) as the criteria remain invariant: I) *Geometry based filter*: deep and sharp defects are more detrimental than shallow and non-sharp defects, irrespective of the loading mode; II) *Linear elastic analysis plus the Theory of Critical distances*: The approach explicitly considers the stress field in the neighbourhood of the defect for the loading mode.

Figure 3 shows the render of the pipeline which provides a clear view of defects within the structure. The tool allows areas of defect density, orientation and dimensions to be calculated, as shown in Fig. 4 and 5. The current analysis focuses only on internal flaws, which is representative for 99.9% of detected defects. Figure 4 also shows that more than 85% of the defects appear in the lower half of the pipeline. Figure 5 shows the distribution of all defects. Only 7.3% of all defects have low sphericity and therefore have a crack-like shape.

The *Geometry based filter* is first applied to the batch data as described in Section 2.1. A graph of Ψ-a/B is constructed using the raw ILI data (1750 anomalies), Fig 6. The most severe screening would only consider the deepest (highest a/B) and flattest (lowest Ψ) flaws. The least conservative approach would be to select those flaws highlighted in the figure joined by a green line; this reduces the number of pits requiring further consideration to only 4. However, for increased conservatism, it may be appropriate to select more of the deeper and flatter pits as shown by the blue (15 pits) and red (43 pits) selections. Clearly, the number of pits that will require more detailed analysis is significantly reduced by the application of this procedure. The analyst can use different criteria to select those pits that will be further analysed in Step 2. The selection criteria depend on user experience and expertise, the potential modes of failure (fatigue, corrosion, etc.), asset criticality, risk of asset failure, company integrity management policies, uncertainty in input parameters, etc. It will be seen below that the elastic analysis in Step 2 can also be used to

inform the selection process in an iterative manner.

The *Theory of Critical Distances* is applied next. Defects within the structure are analysed by means of elastic FEA. For simplicity, the analysis carried out in this paper is that for the least conservative selection of 4 pits in Step 1; those pits shown in Fig. 6 joined by the green line. In general terms the analyses to follow are the same, regardless of the number of pits that have gone through to this step.

Figure 7 shows the location and orientation of defects in the pipeline and results of the elastic stress analysis for an applied internal pressure (P=35 MPa) for the four defects selected in Step 1. The maximum opening stress field at the symmetry plane, normalised by the opening stress field remote from the defective area, for each of the four pits and the application of the PM to evaluate stresses at the critical distance ($L/2$) are shown in Fig. 8. A number of observations may be made from this figure.

- First, it is readily observed that Pit 2 (blue curve) and Pit 3 (red curve) have the more severe elastic stress fields, followed by Pit 1 (pink curve) and Pit 4 (black curve), respectively.
- Secondly, the ranking of defects in terms of severity is not strongly dependent on the value of L.
- Finally, the analyses suggest that selection of additional pits to be analysed should be in the surrounding area of pits 2 and 3, as shown in Fig. 9 (green rectangle).

This last point represents an iterative process between Steps 1 and 2 of the screening approach. If any additional pits selected lead to higher elastic stresses, then the selection process can be extended further. If not, the selection process can be terminated and the assessment proceeds to Step 3. Note, it is not intended that Pit 1 and Pit 4 are excluded from Step 3; at Step 3, pit 1 being the most crack-like may be found to be more susceptible to fracture and pit 4 being the deepest may be found to be more susceptible to plastic collapse. The outcome of Step 3 may, therefore, also lead to iteration with the screening steps and the selection of more pits.

The orientation of defects with respect to the load direction is not considered in the geometry based filter; that is why the value of the critical stress (σ_{cr}^{Pit}) does not have a clear trend with respect to the value of Ψ-a/B in Fig. 8. Nevertheless, the approach does consider orientation in the elastic analysis where two pits of the same geometry (same Ψ-a/B), one being unfavourably (w.r.t. the loading) oriented and the other being in a more favourable (i.e. parallel to the loading direction) orientation are ranked differently.

The above analysis has only considered 4 pits and iteration would likely lead to selection of a larger number for detailed analysis. A second example with

the same dataset is used here to show how considering orientation can be used to reduce the number of pits selected. Figure 10(a) shows a possible selection of defects by the analyst at Step 1, where points (86 solid circles) below the blue line are considered to require further analysis. Figure 10(b), showing the aspect ratios a/c and a/l as a function of normalized pit depth, is constructed for these defects. Only defects with the lowest a/c and a/l ratios for given values of a/B are selected for further analysis. This selection is based on the standard stress intensity factor solutions for defects under pressure, shown in Fig. 11(a) and Fig. 11(b) for circumferential and axial cracks, respectively, which demonstrate that the stress intensity factor reduces with increasing a/c or a/l for given a/B.

As a result, 42 flaws out of 86 would be selected for more detailed analysis by means of elastic FEA (Step 2). These flaws are shown in Fig. 12 in semi-solid blue circles.

4 Discussion

The approach proposed in this paper aims to increase the efficiency of integrity assessments when there is a large inspection area and the large number of detected anomalies prevents the application of detailed, advanced fitness-for-service approaches to all anomalies. The method uses the geometry of defects as a first step in reducing the amount of inspection data. The geometry is assessed by the use of: (a) sphericity, quantifying the degree of flattening of the defected flaws, (b) depth relative to section thickness, which is key factor in both plastic collapse and fracture based assessments, and (c) aspect ratios which has been shown to strongly influence elastic stress intensity factor solutions. However, geometry is not the only consideration: a second step in the screening approach uses elastic stress analysis and a simple point method to rank flaws. The stress analysis step may be used with the geometry based step in an iterative manner to increase or decrease the number of anomalies requiring detailed analysis.

It is worth noting that while sphericity provides important information regarding the deviation of defects from spherical shape as it accounts both for form (three-dimensionality of a flaw) and roundness (angularity or sharpness), it has been recognised [38] that it can only be used rigorously in conjunction with the use of additional shape factors or aspect ratios to remove ambiguity, i.e two defects of different shape can be of the same volume and with equal surface area. In the proposed approach we have coupled the use of sphericity (Ψ) with depth relative to different directions (a/B, a/c, a/l) to achieve this.

In addition, there are parameters that could be explored to account for surface

features which are small-scale relative to the size of the defect. There has been extensive work in this area, as described by Blott et.al [39], where the use of regularity or surface texture, for example, would allow indentations and the existence of non-smooth surfaces to be included in the analysis as could be potential threats due to their stress/strain concentration characteristic. However, due to inherent limitations of conventional ILI technologies, the level of detail about the geometry of defects is limited. Therefore, currently the use of simple geometry based filtering in conjunction with stress analysis is a pragmatic way forward.

The stress analysis proposed is elastic stress analysis. The analysis should be for the loadings of concern for the component under consideration. Where a pipeline is subjected to pressure, axial load and/or bending, results of the type shown in Fig. 11 support the geometry based filtering based on aspect ratio. However, if other stresses are dominant, then behaviour may be more complex. For example, through-wall thermal stresses may be higher near a surface as may welding residual stresses. Then shallower defects may be of more concern. Thus, it is prudent to select a range of defects in the screening steps and consider iteration with the detailed assessment in Step 3 where the ranking may differ from that produced in Steps 1 and 2.

Detected anomalies that have not passed the screening methodology (i.e. the most severe defects) will require further analysis in Step 3. Such considerations necessitate an understanding of the failure mechanisms involved (e.g, plastic collapse, environmental effects on crack initiation and propagation, fatigue, fracture), the effects on material's behaviour and detailed calculations of local driving forces in the surrounding area of the defect. Such analyses are beyond the scope of this paper but, for illustration, Fig. 13 shows an example in which the elastic-plastic stress and strain fields are evaluated at a service load level. The material true stress-strain data is seen in Table 2. The elastic-plastic stress fields differ from the elastic solutions developed in the screening step but confirm that pit 2 and pit 3 are the most severe flaws. The magnitude of the plastic strains could be used with crack initiation and propagation criteria, such as those developed in [25], to determine whether or not any of the flaws selected in Steps 1 and 2 are likely to grow. Clearly, if all flaws selected are predicted to grow in service, then further defects need to be selected for detailed analysis. However, the overall approach will still allow remaining life estimations for the structure to be made based on the analysis of a reduced number of detected anomalies.

By reducing the amount of defects in Steps 1 and 2, the underlying competition between the intrinsic failure mechanisms can be analysed in detail in Step 3. The method is then appealing for cases in which there is interest in assessing competing mechanisms of failure. For example, the benefit of the proposed method is readily seen in the severity assessment of pit 4. It is shown in Fig.

13 that stresses remain elastic in the vicinity of the defect at the applied load level, thus plastic collapse or fracture are unlikely to occur. However, the re-characterisation process would have envisaged a different scenario, i.e. the analysis of a deep crack-like feature (note the pit 4 has the highest a/B ratio in the analysis), leading to erroneous (or at least over-conservative) decisions. This is the case of corrosion in weld metal, where differences between treating detected defects as crack-like flaws and treating them as loss in load-carrying area are profound, not only in terms of the inherent conservatism and the decisions that would come from each route, but also in terms of the effort and material data required.

Additional issues that could be considered in developing the approach are the defect detection likelihood (probability of detection, probability of identification) achieved and the accuracy of measurements (confidence level). The latter uncertainty could be treated by increasing the sizes of all anomalies prior to application of the screening steps. The use of probabilistic approaches [40–43] to account for the statistical fuzziness of the geometrical inspection could be used together with the scatter in the relevant material properties to yield a more informative analysis in terms of probability of failure. However, to achieve this, knowledge about the real statistical distributions in ILI data is required and the screening steps would need to sample a sufficient number of anomalies for the detailed analyses in Step 3 to provide a reasonable estimate of overall failure probability.

5 Conclusions

A rendering tool has been developed to allow structural integrity analysts of pipelines to have a clearer view of defects, providing simplified procedures to analyse defect population, reduce ILI data, extract FEA models of the defective pipeline and evaluate the criticality of defects.

The main objective of the proposed method has been to reduce the amount of data requiring detailed analysis from that obtained during in-line-inspection. To achieve this, a *Geometry based filter* consisting of two parts is first applied. The first part is based on the pit sphericity (Ψ) and pit depth to thickness ratio (a/B). The second part is based on pit aspect ratios, reflecting the increased driving force of defects being dependent on the shapes of the projected area of the defect on the circumferential and axial planes of the pipeline wall.

Following the geometry based step, the *Theory of Critical Distances* is applied as a simple and consistent approach to generate a ranking of flaws. For a particular case of in-field data, it was shown that the number of pits requiring detailed analysis in a 12.75 inch riser of 11 km length could be reduced signif-

icantly, depending on the level of conservatism used in the initial selection.

The proposed approach will contribute to reducing the amount of analysis required of data collected during in-line inspection and will allow the analysis to focus only on problematic pits, to assess the pipeline condition and establish if repair, maintenance or a change to the operating conditions is required. The approach has been illustrated through an example from the oil and gas industry, but could potentially be applied to other structures affected by corrosion such as marine structures. Finally, it is expected that the rendering tool will also be useful to display the evolution of defects within a pipeline from different inspections, allowing for improved assessment of growth with time.

Acknowledgments

The authors would like to acknowledge the funding and technical support from BP through the BP International Centre for Advanced Materials (BP-ICAM) which made this research possible. Financial support from the International Campus of excellence (ICE) Andalucia TECH is also greatly acknowledged.

References

[1] Vanaei H.R. , Eslami A. , Egbewande A., 2017. A review on pipeline corrosion, in-line inspection (ILI), and corrosion growth rate models. *International Journal of Pressure Vessels and Piping*, **149**, pp. 43–54.

[2] Barbian A., Beller M., 2008 In-line inspection of high pressure transmission pipelines: state of the Art and Future Trends. In: 81th world conference on nondestructive testing, durban, South Africa. p. 81.

[3] Anderson T.L., 2007. Recent advances in fitness-for-service assessment. *Proceedings of the 4^{th} middle East Nondestructive Testing Conference and Exhibition.*

[4] ASME B31G, Manual for Determining the Remaining Strength of Corroded Pipelines, 2012.

[5] API 579/FFS1, American petroleum institute: Recommended practice for fitness-for-service, 2015.

[6] Recommended Practice - DNV RP-F101 Corroded Pipelines, 2015.

[7] BS 7910: Guide on methods for assessing the acceptability of flaws in metallic structures. British Standards Institution; 2013

[8] Wang WQ, Li AJ, Li PN, Ju DY., 1994. Engineering approach for notch elastic-plastic fracture analysis *International Journal of Pressure Vessels and Piping* **60**, pp. 1-16.

[9] Smith E. 1999. Fracture initiation at the root of a blunt flaw: description in terms of Kr-Lr failure assessment curves. *International Journal of Pressure Vessels and Piping* **76**, pp. 799-800.

[10] Matvienko Y.G., 2003. Local fracture criterion to describe failure assessment diagrams for a body with a crack/notch. *International Journal of Fracture***124**, pp. 107-12.

[11] Cicero S, Gutierrez-Solana F, Horn AJ., 2009 Experimental analysis of differences in mechanical behaviour of cracked and notched specimens in a ferritic-pearlitic steel: Considerations about the notch effect on structural integrity. *Engineering Failure Analysis* **16**, pp. 2450-66.

[12] Horn A. and Sherry A., 2010. Prediction of cleavage fracture from non-sharp defects using the weibull stress based toughness scaling model. *International Journal of Pressure Vessels and Piping,* ***87***(12), pp. 670–680.

[13] Horn A. and Sherry A., 2012. An engineering assessment methodology for non-sharp defects in steel structures-part I: Procedure development. *International Journal of Pressure Vessels and Piping,* ***89***, pp. 137–150.

[14] Cicero S., Madrazo V., Garcia T., Cuervo J., Ruiz E., 2013 On the Notch Effect in Load Bearing Capacity, Apparent Fracture Toughness and Fracture Mechanisms of Polymer PMMA, Aluminium Alloy Al7075-T651 and Structural Steels S275JR and S355J2. *Engineering Failure Analysis* **29**,pp. 108-121.

[15] Hamid Z.M.A., Bae K.-H.,Youn G.-G.,Lee D.-Y., Kim Y.-J. and Kamaya, M., 2015. Fracture mechanics study on the effects of various notch radii by using FE analysis. *ASME 2015 Pressure Vessels and Piping Conference, PVP2015-45749*

[16] Han, J.-J., Larrosa, N. O., Kim, Y.-J., and Ainsworth, R. A., 2015. Blunt defect assessment in the framework of the failure assessment diagram. *International Journal of Pressure Vessels and Piping* **146**, pp. 39–54.

[17] Brown G. W., Parietti L., Rose B., and Anderson T.L., 2016. Evaluation of groove radius assessment criteria based on brittle and ductile local failure models. *ASME 2016 Pressure Vessels and Piping Conference, PVP2016-63756.*

[18] Kim J.S., Larrosa N.O., Horn A.J., Kim Y.-J., Ainsworth R.A., 2017. Notch Bluntness Effects on Fracture Toughness of a Modified S690 Steel at 150^{O}C. *Engineering Fracture Mechanics*. In press.

[19] Betegon C. and Hancock J. W., 1991. Two-parameter characterization of elastic-plastic crack-tip fields. *Journal of Applied Mechanics, Transactions ASME*, 58(1):104–110.

[20] O'Dowd N.P. and Shih C.F., 1991. Family of crack-tip fields characterized by a triaxiality parameter-I. Structure of fields. *Journal of the Mechanics and Physics of Solids*, 39(8):989–1015.

[21] Pineau A., 2006. Development of the local approach to fracture over the past 25 years: Theory and applications. *International Journal of Fracture*, 138(1-4):139–166.

[22] Ruggieri C. and Dodds Jr. R.H., 1996 A transferability model for brittle fracture including constraint and ductile tearing effects: A probabilistic approach. *International Journal of Fracture*, 79(4):309–340.

[23] Bao Y. and Wierzbicki T.,2004. On fracture locus in the equivalent strain and stress triaxiality space. *International Journal of Mechanical Sciences*, 46(1):81–98.

[24] Bao Y., 2005. Dependence of ductile crack formation in tensile tests on stress triaxiality, stress and strain ratios. *Engineering Fracture Mechanics*, 72(4):505–522.

[25] Oh C.-S., Kim N.-H., Kim Y.-J., Baek J.-H., Kim Y.-P. and Kim W.-S., 2011. A finite element ductile failure simulation method using stress-modified fracture strain model. *Engineering Fracture Mechanics*, 78(1):124–137.

[26] Han J.-J., Larrosa N.O, Ainsworth R.A. and Kim Y.-J., 2016. The use of SE(T) specimen fracture toughness for FFS assessment of defects in low constraint conditions. *Procedia Structural Integrity, 2*, pp. 1724 – 1737. 21st European Conference on Fracture, ECF21, 20-24 June, Catania, Italy.

[27] Larrosa, N.O, and Ainsworth, R.A, 2017. A transferability approach for reducing excessive conservatism in fracture assessments. *Engineering Fracture Mechanics*, 174: 54-63

[28] Rusk D.T and Hoppe W., 2009 Fatigue life prediction of corrosion-damaged high-strength steel using an equivalent stress riser (ESR) model. Part I: Test development and results *International Journal of Fatigue*, 31 (10), pp. 1454-1463.

[29] Rusk D.T and Hoppe W., Braisted W. and Powar N., 2009. Fatigue life prediction of corrosion-damaged high strength steel using an equivalent stress riser (ESR) model. Part II: Model development and results *International Journal of Fatigue*, 31 (10), pp. 1464-1475.

[30] Burns J.T. , Larsen J.M. , and Gangloff R.P., 2011. Driving forces for localized corrosion-to-fatigue crack transition in Al-Zn-Mg-Cu. *Fatigue and Fracture of Engineering Materials and Structures*, 34(10):745–773.

[31] Xu S.-H. and Wang Y.-D., 2015. Estimating the effects of corrosion pits on the fatigue life of steel plate based on the 3D profile. *International Journal of Fatigue*, 72, pp. 27-41.

[32] Larrosa N.O., Chapetti M.D. and Ainsworth R.A., 2016. Fatigue life estimation of pitted specimens by means of an integrated fracture mechanics approach. *ASME 2016 Pressure Vessels and Piping Conference, PVP2016-63888.*

[33] Wadell H., 1932. Volume, shape and roundness of rock particles. *Journal of Geology*, 40 (5), pp. 443-451.

[34] *ABAQUS V. 6.10, Reference Manual, Simulia, Dassault Systemes, 2010.*

[35] Taylor D., 1999 Geometrical effects in fatigue: a unifying theoretical approach. *International Journal of Fatigue*, 21(12), pp. 413–420.

[36] Susmel L. and Taylor D., 2008. The theory of critical distances: a review of its applications in fatigue. *Engineering Fracture Mechanics,* ***75***(7), pp. 1706–1724.

[37] Susmel L. and Taylor D., 2008. On the use of the Theory of Critical Distances to predict static failures in ductile metallic materials containing different geometrical features. *Engineering Fracture Mechanics,* ***75***(15), pp. 4410–4421.

[38] Less G. 1964 A new method for determining the angularity of particles. *Sedimentology*, 3 (1), pp. 2-21.

[39] Blott S.J. and Pye K. 2008. Particle shape: a review and new methods of characterization and classification. *Sedimentology*, **55**, pp. 31-63.

[40] Dobmann G., Cioclov D. and Kurz J.H. 2007. The role of probabilistic approaches in NDT defect-detection, -classification, and -sizing. *Welding in the World*, 51 (5-6), pp. 9-15.

[41] Flynn E.B., Todd M.D., Wilcox P.D., Drinkwater B.W. and Croxford A.J. 2011. Maximum-likelihood estimation of damage location in guided-wave structural health monitoring *Proceedings of the Royal Society A: Mathematical, Physical and Engineering Sciences*, 467 (2133), pp. 2575-2596.

[42] Huang Q., Gardoni P. and Hurlebaus S., 2012. A probabilistic damage detection approach using vibration-based nondestructive testing *Structural Safety*, 38, pp. 11-21.

[43] Humeida Y., Wilcox P.D., Todd M.D. and Drinkwater B.W. 2011. A probabilistic approach for the optimisation of ultrasonic array inspection techniques *NDT and E International*, 68, pp. 43-52.

Pipeline length (km)	11
Outer radius (r_0) (mm)	162
Thickness B (mm)	40
Class factor	0.72
Reference pressure (MPa)	69.3
Number of defects detected	1750

Table 1
12.75" riser: main parameters

True strain (mm/mm)	True stress (MPa)
0.00	464.5
0.01	472.50
0.0184	483.34
0.0247	504.67
0.033	526.94
0.0438	550.20
0.058	574.48
0.0767	599.83
0.101	626.30
0.133	653.94
0.1512	665.12
0.1748	682.80
0.2295	712.94
0.3011	744.40
0.3949	777.25
0.5176	811.55
0.6782	847.37
0.8883	884.77
1.1633	923.81
Young's modulus E (GPa)	Poisson's ratio ν
210.7	0.3

Table 2
API X65 material properties for elastic-plastic analysis.

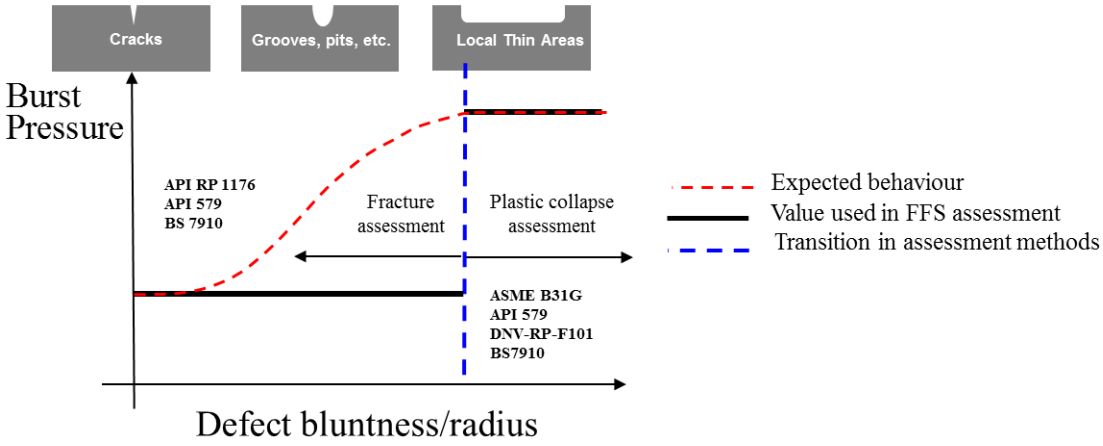

Fig. 1. Effect of notch acuity on burst pressure and treatment of detected defects in fitness-for-service codes. Figure adapted from [17].

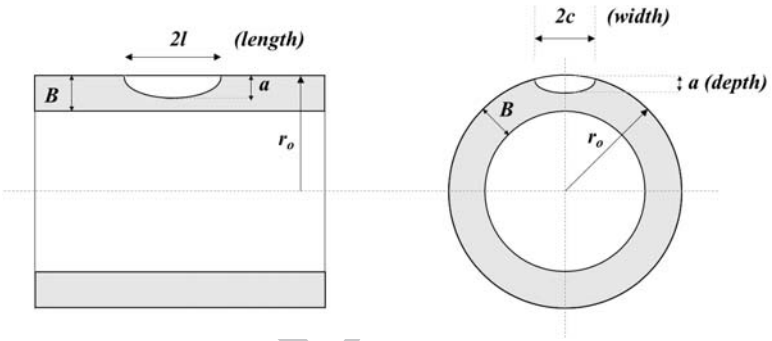

Fig. 2. Defect and pipe relevant dimensions.

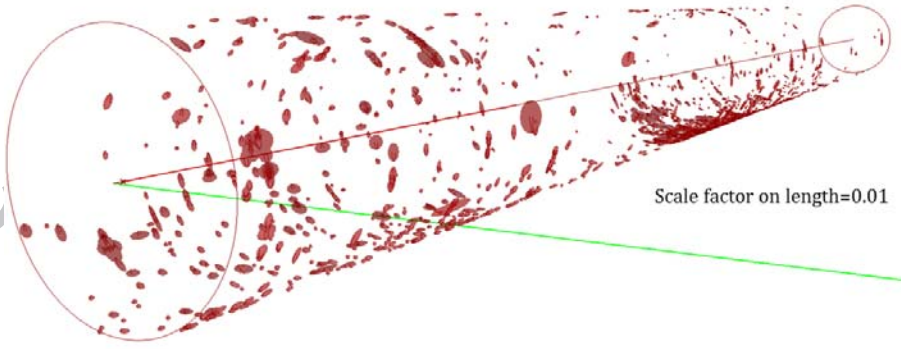

Fig. 3. Visualisation of defects in the pipeline as outcome from the rendering tool.

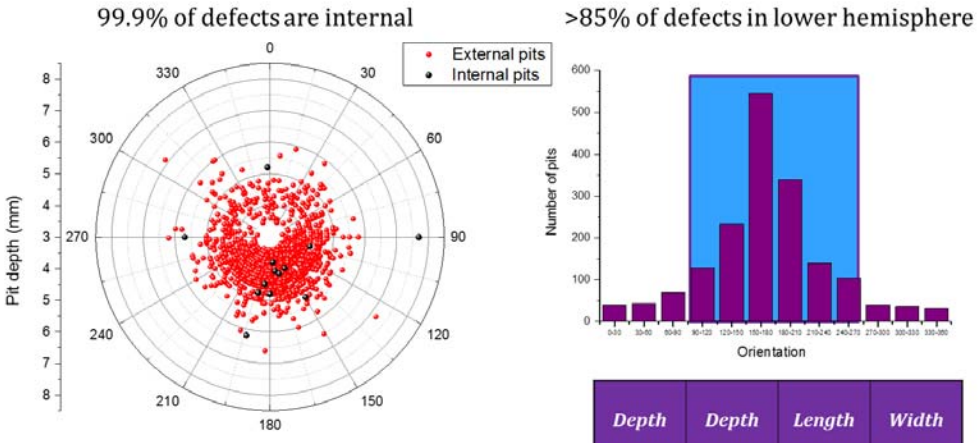

	Depth (mm)	Depth (%)	Length (mm)	Width (mm)
Min	3.40	10.00	5.08	5.08
Max	7.70	19.60	172.7	78.74
Mean	4.24	11.38	17.02	11.94
Std. Dev	0.53	1.23	18.29	8.13

Fig. 4. Analysis of defect geometry and location.

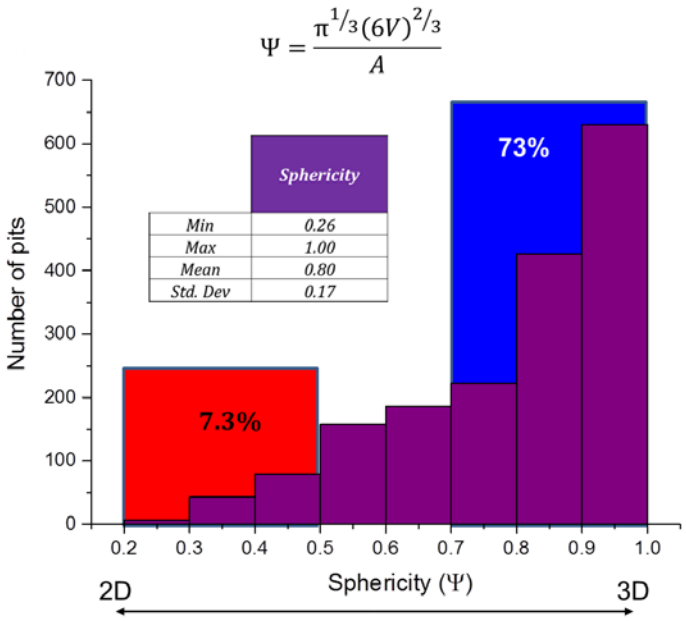

Fig. 5. Roundness (sphericity) of defects encountered at riser.

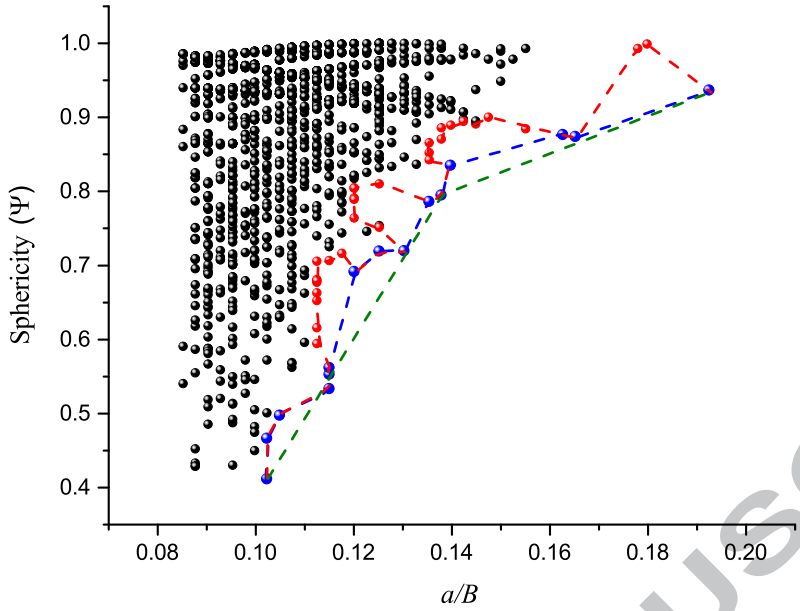

Fig. 6. Step 1: Sphericity Vs. normalised depth of defects. Different criteria with varying levels of conservatism are shown.

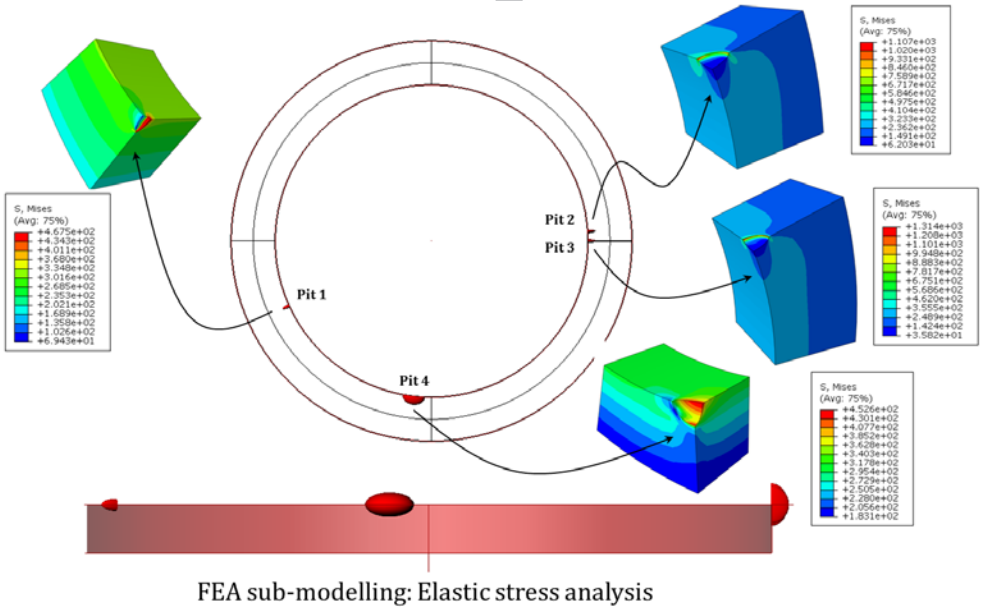

Fig. 7. Step 2: Sub-modelling approach, elastic finite element analysis.

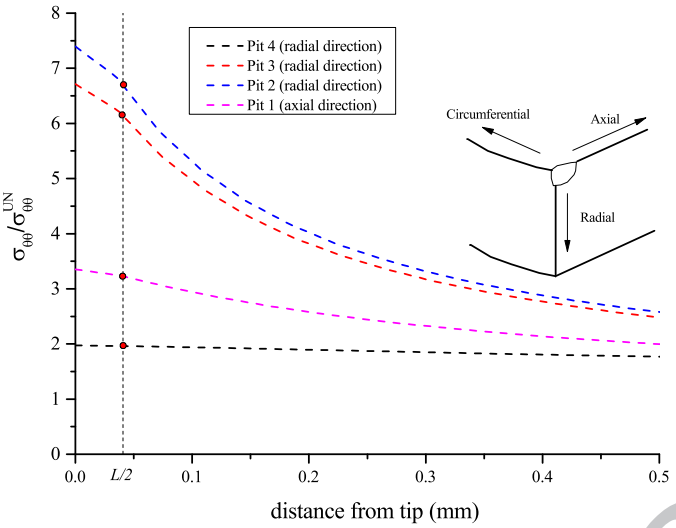

Fig. 8. Step 2: Normalised elastic opening stress and application of the Point Method (PM) to rank pits. $\sigma_{\theta\theta}^{UN}$=124.25 MPa is circumferential stress in the non-defective component for P=35 MPa

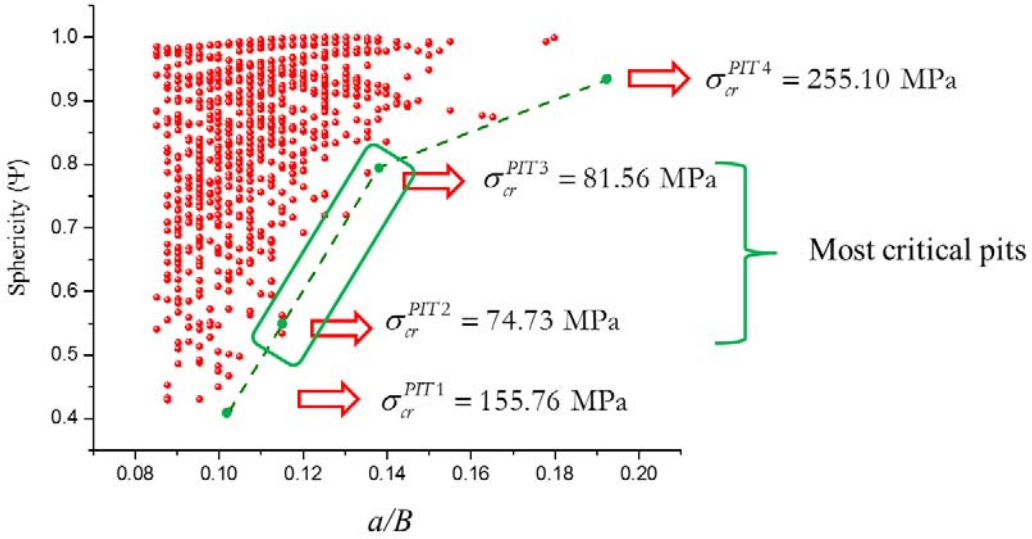

Fig. 9. Step 2: Rank of pits and zone in which pits can be further analysed. $\sigma_{cr} = \Delta\sigma_{FL}$=500 MPa, R=0.5.

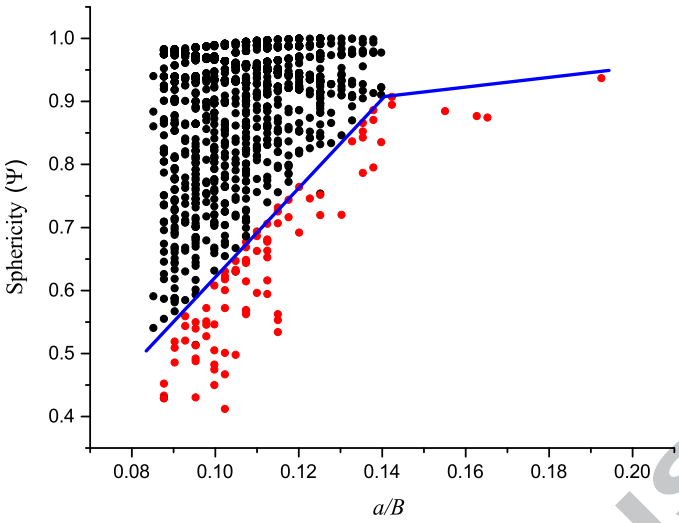

(a) Arbitrary selection of defects by the analyst.

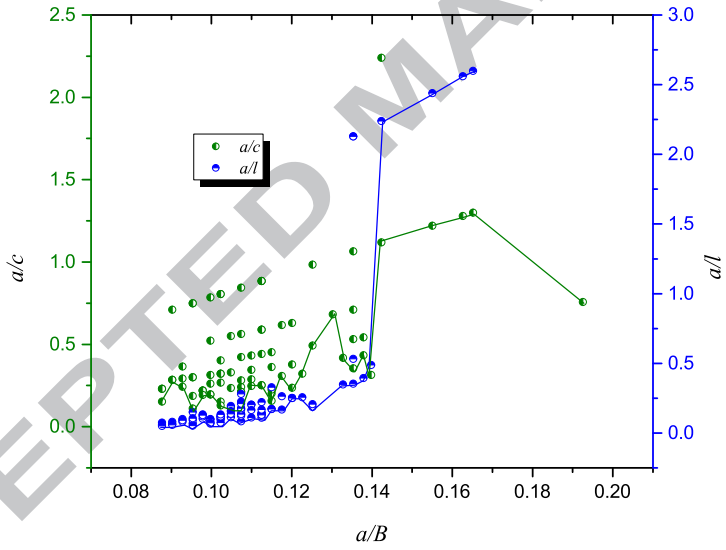

(b) Aspect ratios of axial (a/l) and circumferential (a/c) projected areas of 3D flaws.

Fig. 10. Arbitrary selection of points by the analyst (red) and double-Y plot to reduce dataset based on aspect ratios a/c and a/l of projected areas of flaws.

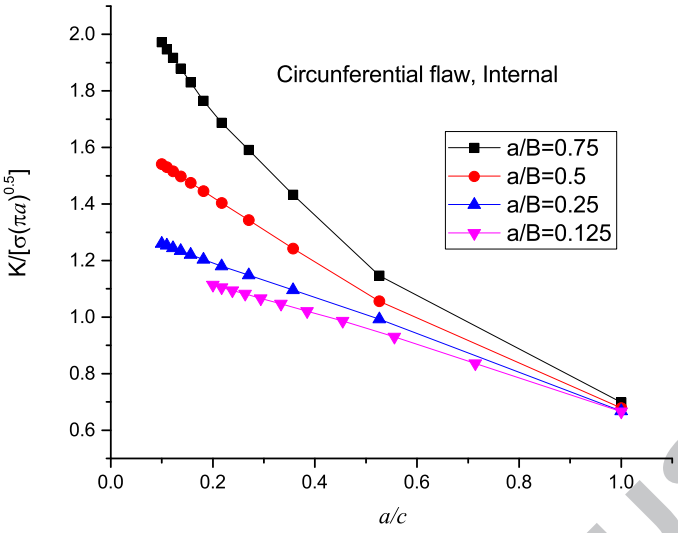

(a) Circumferential cracks.

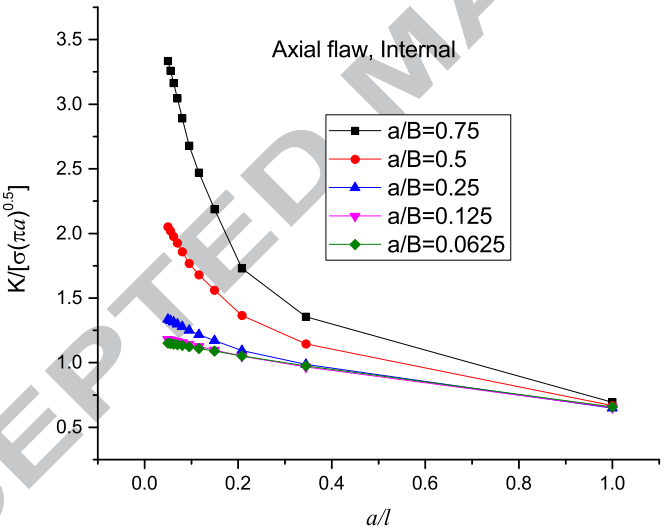

(b) Axial cracks.

Fig. 11. *Normalised SIF Vs. crack aspect ratio* for internal cracks in cylinders under internal pressure.

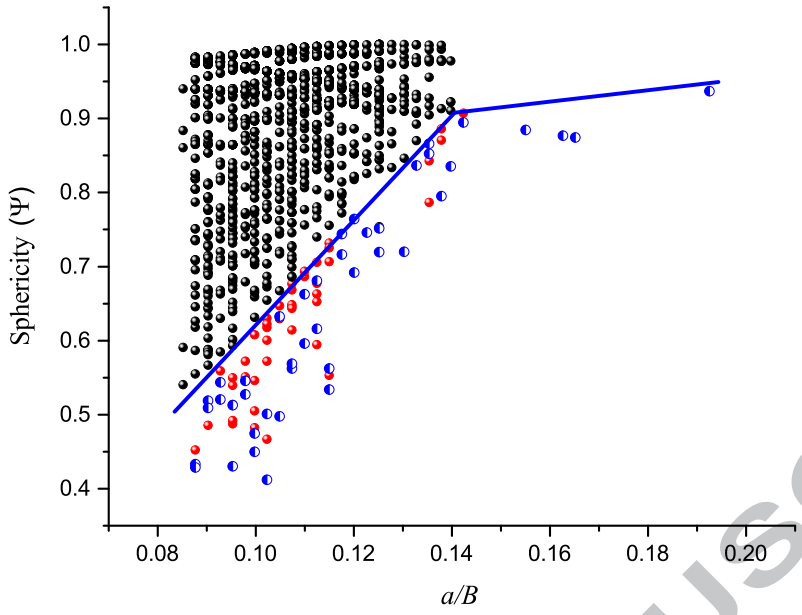

Fig. 12. Arbitrary selection of points by the analyst (red) and reduced dataset using aspect ratios a/c and a/l of projected areas of defects (semi-solid blue).

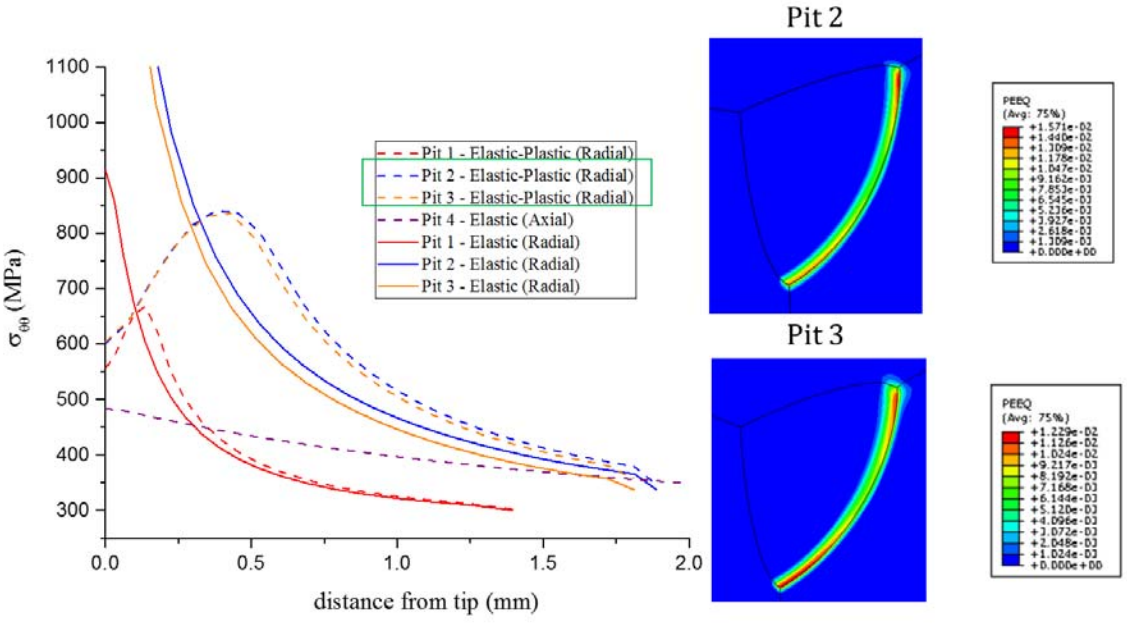

Fig. 13. Elastic and Elastic-plastic stress and strain analyses.

Highlights:

- The proposed method reduces the amount of data requiring detailed analysis from that obtained during inline- inspection of Oil and Gas pipelines.

- The procedure uses a geometry-based filter and finite elements elastic stress analysis to identify most severe flaws.

- A rendering tool allows a clear view of defects within the structure, evaluate dimensional parameters and allow FEA models to be extracted.